SCIENTIFIC REPORTS

OPEN

SUBJECT AREAS:
GRAPHENE
APPLIED PHYSICS
ELECTRONIC PROPERTIES AND DEVICES

Received
22 April 2014

Accepted
15 July 2014

Published
11 August 2014

Correspondence and requests for materials should be addressed to T.-L.R. (RenTL@tsinghua.edu.cn); J.X. (JunXu@Tsinghua.edu.cn) or L.-J.L. (lance.sinica@gmail.com)

* These authors contributed equally to this work.

Novel Field-Effect Schottky Barrier Transistors Based on Graphene-MoS_2 Heterojunctions

He Tian[1,2]*, Zhen Tan[1,2]*, Can Wu[1,2]*, Xiaomu Wang[1,2]*, Mohammad Ali Mohammad[1,2], Dan Xie[1,2], Yi Yang[1,2], Jing Wang[1,2], Lain-Jong Li[3], Jun Xu[1,2] & Tian-Ling Ren[1,2]

[1]Institute of Microelectronics, Tsinghua University, Beijing 100084, China, [2]Tsinghua National Laboratory for Information Science and Technology (TNList), Tsinghua University, Beijing 100084, China, [3]Physical Science and Engineering division, King Abdullah University of Science and Technology, Thuwal 23955-6900, Saudi Arabia.

Recently, two-dimensional materials such as molybdenum disulphide (MoS_2) have been demonstrated to realize field effect transistors (FET) with a large current on-off ratio. However, the carrier mobility in backgate MoS_2 FET is rather low (typically 0.5–20 $cm^2/V{\cdot}s$). Here, we report a novel field-effect Schottky barrier transistors (FESBT) based on graphene-MoS_2 heterojunction (GMH), where the characteristics of high mobility from graphene and high on-off ratio from MoS_2 are properly balanced in the novel transistors. Large modulation on the device current (on/off ratio of 10^5) is achieved by adjusting the backgate (through 300 nm SiO_2) voltage to modulate the graphene-MoS_2 Schottky barrier. Moreover, the field effective mobility of the FESBT is up to 58.7 $cm^2/V{\cdot}s$. Our theoretical analysis shows that if the thickness of oxide is further reduced, a subthreshold swing (SS) of 40 mV/decade can be maintained within three orders of drain current at room temperature. This provides an opportunity to overcome the limitation of 60 mV/decade for conventional CMOS devices. The FESBT implemented with a high on-off ratio, a relatively high mobility and a low subthreshold promises low-voltage and low-power applications for future electronics.

Graphene, a two dimensional material, has attracted much attention due to its outstanding properties[1,2], such as ultrahigh mobility[3], mechanical strength[4], thermal conductivity[5] and transparency[6]. However, the zero bandgap of graphene limits its applications in electronics. Different forms of graphene such as graphene nanoribbons[7,8], bilayer graphene[9,10] and graphene oxide[11,12] have been reported to possess a bandgap. However, the typical switching ratios of the devices based on these structures is still lower than 10^3. Recently, MoS_2 is used to realize transistors with a large I_{on}/I_{off} ratio. However, the mobility of MoS_2 in the back gate FET structure is rather low (typically 0.5–20 $cm^2/V{\cdot}s$)[13–16]. Most recently, an important milestone is the creation of heterostructures based on graphene and other two-dimensional crystals[17–20]. L. Britnell et al.[18] used molybdenum disulfide as a vertical transport barrier to realize a graphene tunneling transistor with a switching ratio $\sim10^4$. Yu et al.[21] fabricated a vertically stacked heterostructure formed by MoS_2 and graphene, which has an on-off ratio of 10^3. Graphene-MoS_2 heterostructures were also demonstrated to work as ultrahigh-gain[20] and high quantum efficiency[22] phototransistors. In addition, nonvolatile memory cells were made based on graphene/MoS_2 heterostructures[23,24]. Most recently, graphene-MoS_2 hybrid structures were demonstrated to work as multifunctional photoresponsive memory devices with a photo responsivity of up to 5×10^8 A/W[25], which is the highest to date among the graphene-based photodetectors.

In order to form the heterojunction between graphene and MoS_2, there are mainly two methods. One is using large-area CVD-grown graphene combined with exfoliated MoS_2[26]. The other is called mechanical transfer technology[18] using exfoliated graphene transferred onto the exfoliated MoS_2. Both of these methods need PMMA to assist in the transfer, which could introduce photoresist contamination. In the formation of the 2D heterojunction, the interface between graphene/MoS_2 is key. In order to obtain a clean interface between graphene and MoS_2, a random exfoliating method is used by first exfoliating MoS_2 followed by exfoliating graphene. After the exfoliation, optical microscopy combined with Raman spectroscopy is used to find the desired graphene/MoS_2 heterojunction. The main advantage of such a method is that there is no PMMA involved in the graphene/MoS_2 heterojunction fabrication process and the interface between both layers are of pristine quality.

We report a novel field-effect Schottky barrier transistor based on graphene-MoS_2 heterojunction (GMH), where the two-dimensional Schottky junction forms between the mechanically exfoliated graphene and MoS_2.

Figure 1 | A gate controlled graphene-MoS_2 heterojunction (GMH). (a) A schematic diagram to show the field-effect Schottky barrier transistor (FESBT) device structure of the gate controlled GMH. (b) The Raman spectrum of the GMH, confirming the formation of the heterojunction between micromechanical exfoliated graphene and MoS_2. The inset shows the laser spot (Red dot) located at the GMH. (c) Optical image of the GMH after the electrode fabrication process. The electrical contacts on MoS_2 and graphene were fabricated by electron beam lithography and electron beam evaporation of Cr/Au (10 nm/50 nm). (d) AFM image of the GMH. The MoS_2 is ~8 nm and graphene is ~3 nm. The graphene is partly folded. The inset shows the graphene-MoS_2 heterojunction with 1 μm^2 area.

The combination of graphene and MoS_2 allows for unprecedented current modulation of $\sim 1 \times 10^5$ at room temperature and a high mobility up to 58.7 $cm^2/V \cdot s$. A MoS_2-graphene-MoS_2 FESBT based on two GMHs is also demonstrated, which has an ability to rectify a current by changing the gate voltage. Our FESBT is fundamentally different from the conventional Schottky barrier FETs[27,28]. In our device, the Fermi level of graphene is tunable by gate voltage since the graphene is a semi-metal with a low density of states[29]. As a result, the Schottky barrier height between graphene and MoS_2 can be modulated. In contrast, the work function of the metal in conventional Schottky barrier FETs is not tunable by field effect. Our device is also quite different from the graphene-MoS_2-graphene tunneling transistors[18]. In Ref. 18, the graphene-MoS_2-graphene device is a kind of tunneling transistor in which the MoS_2 serves as a barrier layer between two graphene layers. Since both graphene and MoS_2 are single-layer, it is easy to observe the tunneling effect. However, in our device, the MoS_2 and graphene layers are thicker (larger than five layers). As a result, the few-layer MoS_2 and graphene can form the Schottky junction with the depletion layer in MoS_2. In this paper, several important observations are reported. Firstly, a large modulation of the device current (on/off ratio of 10^5) is achieved by adjusting the back gate voltage (through 300 nm SiO_2) to control the graphene/MoS_2 Schottky barrier. Secondly, theoretical analysis shows that the subthreshold swing of FESBT can be as low as 40 mV/dec, overcoming the limitation of 60 mV/dec present in conventional field-effect transistors[30]. This is a breakthrough in field-effect transistors. Thirdly, a high mobility up to 58.7 $cm^2/V \cdot s$ is achieved, which is higher than previously reported back-gated MoS_2 transistors. Finally, a novel MoS_2-graphene-MoS_2 FESBT is also demonstrated which has an ability to rectify a current by changing the gate voltage. This shows the concept that we can switch between "diode" and "resistor" easily, which could pave the way for various applications in electronics systems.

Results

A gate controlled graphene-MoS_2 heterojunction. Figure 1a illustrates the schematic structure of a FESBT device. The contact between graphene and MoS_2 forms a Schottky junction, which is the core part of the device. The drain electrode is connected to MoS_2 to apply bias voltage (V_d), while the source is grounded with graphene. The fabrication and basic characterization procedures of FESBT are described briefly. At first, few-layers MoS_2 and graphene flakes were in turn mechanically exfoliated onto N^+ doped silicon substrates covered with 300-nm-thick SiO_2. Raman spectroscopy was performed to confirm the locations of graphene and MoS_2, as well as their junctions (Figure 1b). Subsequently, the metal contacts to MoS_2 and graphene were fabricated using electron beam lithography and electron beam evaporation of Cr/Au (10 nm/50 nm)

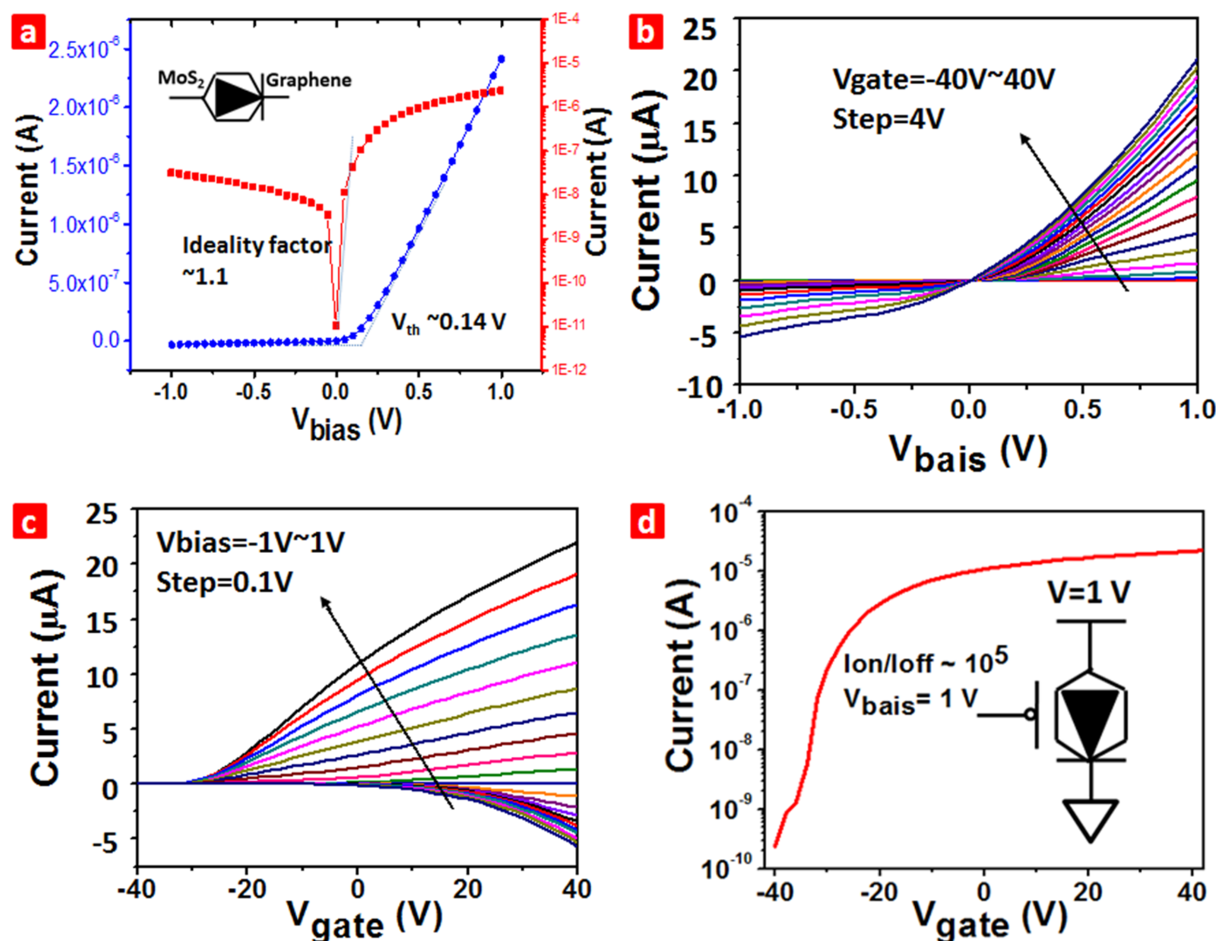

Figure 2 | The experimental results of the gate controlled GMH. (a) Current vs. bias voltage characteristic of a GMH (V_{gate} = 0), showing a Schottky diode characteristic with ~1.1 ideality factor. (b) The current vs. bias voltage characteristics of GMH at various V_{gate}. The black arrow indicates the direction of increasing V_{gate}. (c) The current vs. gate voltage characteristics of GMH at various V_{bias}. The black arrow indicates the direction of increasing V_{bias}. (d) The forward bias current as a function of V_{gate}. A unipolar control of forward current with the ratio of 10^5 is obtained.

(Figure 1c). The thicknesses of MoS_2 and graphene are ~8 nm and ~3 nm respectively, as determined by AFM measurements in Figure 1d. The overlapping area of MoS_2 and graphene is about 1 μm^2.

The forward characteristics at a low bias voltage show a diode ideality factor of ~1.1 (Figure 2a). When the bias voltage is ramped from 0 to 0.05 V, the current increases by three orders of magnitude. This indicates that the measured current may be due to tunneling between graphene and MoS_2. Moreover, such a low threshold voltage (V_{th} ~ 0.14 V) of GMH is promising for low-voltage operation. Figure 2b shows the output characteristics (I_d-V_g) at different gate voltages (V_g). These results show a pronounced increase in conductance with increasing V_g. The change of the current flow is due to the modification of Schottky barrier height by gate voltage. The transfer characteristics at different drain voltages is shown in Figure 2c. For the FESBT the largest current density is about 2,400 A/cm^2 obtained with V_g = 40 V and V_d = 1 V. The transfer curve in Figure 2d, plotted on a log scale, shows that the FESBT exhibits a ~10^5 on-off ratio with the gate voltage ranging from −40 V to 40 V. Note that a 300-nm-thick SiO_2 is used as back gate oxide in our device. As shown in figure S3, the on/off ratio of the GMH device (10^5) is much higher than that of the same MoS2 flake (944) used in our device. Accordingly, we conclude and emphasize that the Schottky junction is responsible for the higher on/off ratio. The ability of the gate control as well as the subthreshold swing (SS) should be further enhanced if a thinner oxide or high-κ dielectric is introduced, which will be discussed later in more detail. We estimate the field effective mobility of FESBT by $\mu_{FE} = \frac{Lg_m}{WC_{ox}V_d}$, where L, W, C_{ox} and g_m are the channel length, width, gate capacitance per area, and the transconductance that is defined by $g_m = \frac{\partial I_d}{\partial V_g}$ at a constant V_d, respectively. Note that since both MoS_2 and graphene were obtained by mechanical exfoliation, the shapes are irregular. As shown in Figure 1d, we evaluated the channel length (L) to be 1.3 μm and the width (W) to be 600 ~ 900 nm. The error bars are used for mobility extraction. To benchmark the performance of FESBTs, the electrical measurement results for the transistors based on pristine graphene and MoS_2 flakes are shown in Figures S1 ~ S4 in the supporting information. Interestingly, the mobility values for the transistors based on pristine graphene and MoS_2 flakes are around 179.7 and 6.5 cm^2/V·s, respectively. Here the mobility of the transistors based on the MoS_2 flakes is significantly lower than the 58.7 cm^2/V·s mobility of the FESBT device. It has been widely reported that MoS_2 is a n-type material, which is corroborated by the high threshold voltage ~18 V as shown in Figure S3, where the current has not saturated even at V_g = 40 V. This is unfavorable for the operation of logic electronics and the mobility extracted from the linear regime could be underestimated. We notice that the threshold voltage of a FESBT is shifted to a negative gate voltage. The core of our device is laid on the Schottky junction and the current modulation is implemented through the sufficient control of the Schottky

Figure 3 | The experimental results of the MoS_2-Graphene-MoS_2 FESBT (MGM-FESBT). (a) Schematic structure of the MGM-FESBT based on two graphene-MoS_2 heterojunctions. (b) Optical image of the MGM heterojunction with few-layer MoS_2 film and few-layer graphene film deposited onto a 300 nm SiO_2/Si substrate. (c) AFM image of the MGM heterojunction. (d) The current vs. bias voltage characteristics of MGM-FESBT at various V_{gate}. The black arrow indicates the direction of increasing V_{gate}. (e) The current vs. gate voltage characteristics of MGM-FESBT at various V_{bias}. (f) The current vs. bias voltage characteristics demonstrating how current can be rectified by changing V_{gate}.

barrier height. The shift of the threshold voltage is attributed to the new working principle of our device.

A gate controlled MoS_2-Graphene-MoS_2 heterojunction. A novel MoS_2-graphene-MoS_2 FESBT (MGM-FESBT) is also demonstrated, which has an ability to rectify a current by changing the gate voltage. As shown in Figure 3a, the structure of the MGM-FESBT consists of two GMHs. Optical microscopy (Figure 3b) and AFM images (Figure 3c) show the structure of the MGM heterojunction. The thicknesses of the two MoS_2 flakes are 40 nm and 24 nm, respect-

ively. The graphene flake is 28 nm thick. The electrical characteristics of the two MoS_2-graphene junctions show some differences (Supporting Figure S5) due the difference of thicknesses of MoS_2 in two GMHs. The working principle of the MGM-FESBT can be described as follows. A large amount of electrons inject from the drain terminal to MoS_2 and then drift into the graphene. Due to the schottky barrier between MoS_2-graphene and the recombination with holes in graphene, only a fraction of the injected electrons can pass through the graphene and be collected by the MoS_2 at the source terminal. As the work function of the graphene is tunable by the gate voltage, the Schottky barrier between MoS_2-graphene could be tuned from the gate to improved contact. Figure 3d shows the current vs. bias voltage characteristics of MGM-FESBT at various V_{gate}. The black arrow indicates the direction of increasing V_{gate}. It indicates that the lower gate voltage can lead to a higher Schottky barrier height between MoS_2 and graphene. Figure 3e shows the current vs. gate voltage characteristics of a MGM-FESBT at various V_{bias}. Figure 3f demonstrates that the barrier property of a MGM-FESBT is tunable by V_{gate}. At $V_{gate} = -10$ V, the Schottky contact is formed in the MGM. After the gate voltage is increased to 42 V, the contact barrier is lowered. This means that the MGM can realize a "diode" to "resistor" transition easily, which may open a wide application space in next generation electronics.

Discussion

The graphene-MoS_2 heterojunction is the core of FESBT devices. In order to fundamentally understand the physics of the heterojunction, a theoretical model is established. As illustrated in Figure 4a, the model consists of three parts: a Schottky junction formed by the GMH and two resistors connected with the source and drain terminals. The electrical performance of our device is mainly dependent on the heterojunction. In this case, the lateral transport is the dominant factor, suggesting that the resistance of this uniform junction is scaled with $L_{junction}/W_{junction}$. Therefore, the junction could also be regarded as an artificial thin film FET. These two resistors are included to consider the resistances of graphene and MoS_2 between the junction and source/drain electrodes. Here MoS_2 is considered as a thin bulk material, and the drop of electric potential in graphene is ignored since it has only several layers. The integral of electric field along the path perpendicular to the plane equals to the difference of work function between MoS_2 and gate, assuming that the electric field is constant in graphene and MoS_2, respectively.

$$F_{ox} \cdot t_{ox} + F_{MoS_2} \cdot t_{MoS_2} = W_{MoS_2} - W_{gate} - V_{ch} \tag{1}$$

where F_{ox/MoS_2}, t_{ox/MoS_2}, $W_{MoS_2} - W_{gate}$, and V_{ch} are the electric field, the thicknesses of the oxide and MoS_2, the difference of the work functions between MoS_2 and gate electrode, and the channel potential of graphene. The electric field is consistent at the interface between the oxide and the MoS_2,

$$F_{ox} \cdot \varepsilon_{ox} = F_{MoS_2} \cdot \varepsilon_{MoS_2} \tag{2}$$

where ε_{ox/MoS_2} is the relative dielectric constant of the oxide and the MoS_2. As the electric field penetrates into graphene, it induces free charges, so we obtain

$$-\varepsilon_{MoS_2} \cdot F_{MoS_2} = e \cdot n_{2D} \tag{3}$$

where e and n_{2D} are electron charge and two-dimensional carrier density in graphene.

For a given Schottky barrier height, assuming only thermionic current for simplicity, the current flow through graphene-MoS_2 heterojunction is evaluated by

$$I = S \cdot A^* T^2 e^{-e\phi_B(V_g)/\eta k_B T}\left(e^{eV_d/\eta k_B T} - 1\right) \tag{4}$$

where S is the effective area of the junction, T is the absolute temperature, ϕ_B is the Schottky barrier modulated by the gate voltage, η is the ideality factor that was extracted from experiments in Figure 2a, and A^* is the Richardson constant, which is expressed by

$$A^* = \frac{4\pi e k_B^2}{h^3}\sqrt{m_x m_y} \tag{5}$$

where h is the Plank constant, and m_x and m_y are the effective masses of electrons. Note that two series resistors of MoS_2 and graphene adjusted by field effect are also included in our model. The detailed discussion about the model is shown in the supporting information.

By solving eq. (1), (2) and (3) above, the Schottky barrier height is obtained at different back gate bias and zero drain voltage. In Figure 4b, it can be seen that the large range of this energy barrier from 0.23–0.57 eV is the main mechanism for gate modulation. In order to demonstrate the validity of this model, the theoretical results are compared with the experimental results, as shown in Figure 4c. Based on this model, we analyze the performance of the FESBT by adjusting the thickness of the oxide and the dielectric constant of the oxide of the device (in the model). As illustrated in Figure 4d, if the effective oxide thickness (EOT) is reduced from 3 nm to 0.39 nm (currently the smallest EOT), the SS factor could be improved from 79 mV/decade to 40 mV/decade, exceeding the limitation of conventional CMOS devices (60 mV/decade). As the operation of convensional transistors is based on the thermionic emission, the sub-threshold swing should not be lower than 60 mV/decade. At present, the only way to realize sub-threshold swing lower than 60 mV/decade is through the tunneling transistor. In our case, since the Schottky junction with depletion layer in MoS_2 is thin, there is partly a tunneling effect where the carriers pass through the graphene/MoS_2 thin Schottky barrier. Moreover, the Schottky barrier (tunneling barrier) could be controlled by the gate voltage, which can realize such a low sub-threshold swing of 40 mV/decade (see supporting information). This interesting result provides useful insights for the future development of FESBT devices. By reducing the thickness of the gate oxide or introducing high-κ dielectric as the gate oxide, the ability of gate control could be greatly enhanced. Additionally, since the lower SS factor offers a sharper turn-on performance for logic circuits, the potential use of FESBT devices seems promising in low-power applications in future electronics. In Figure 4e and 4f, we present the extracted mobility as a function of the gate voltage and barrier height, where the error bars for each gate voltage is plotted based on the maximum and minimum values of the junction width.

Based on the above analysis, a clearer working principle may be proposed for our FESBT. The energy level alignment of the FESBT with $Si/SiO_2/MoS_2$/Graphene structure is shown in Figure 5a. Since the affinity energy of MoS_2 (4.15 eV) is smaller than the work function of the Graphene (4.5 eV), the Schottky junction can form. Figure 5b ~ 5d shows how electrons transport through the graphene-MoS_2 Schottky junction in response to the modulation by the gate voltage. As shown in Figure 5b, there is a built-in voltage between Si and MoS_2 after Fermi-level alignment, which could induce dipoles in the oxide. Applying a positive voltage to the gate induces electrons in graphene (Figure 5c), raising its Fermi level and thus decreasing the Schottky barrier height. When a negative voltage is applied to the gate (Figure 5d), it could induce holes in graphene and decrease its Fermi level, leading to the increase in Schottky barrier height. As for the working principle of the MGM-FESBT, the MoS_2-graphene-MoS_2 can be modeled as two Schottky junctions connected back to back. The band diagrams are illustrated in Figures 5e and 5f. When applying a low gate voltage, the Schottky barrier heights for both junctions are large. One of the Schottky junctions is positively biased, and the other is negatively biased. The current is suppressed by the negatively biased one. So the device behaves like a Schottky junction under reverse bias. When applying a higher gate voltage, the Fermi level of graphene rises and the energy barriers of two junctions decrease. Thus the conductance becomes much higher, which makes the device with "improved contact".

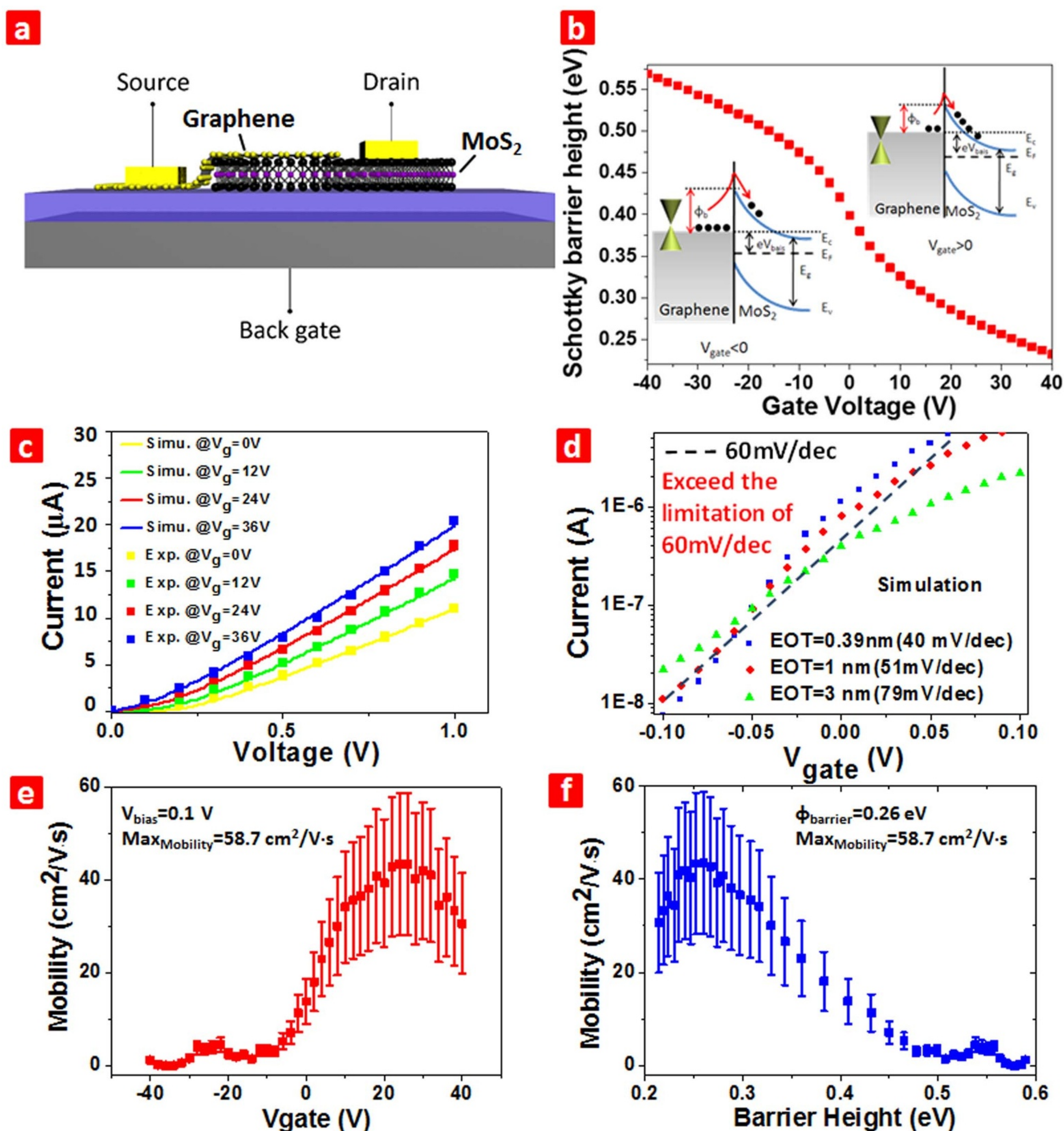

Figure 4 | The theoretical model of the gate controlled GMH. (a) The schematic structure of the gate controlled GMH. The MoS_2 is sandwiched between the graphene and the SiO_2. (b) The Schottky barrier height obtained from different gate bias by solving the Poisson equation. Large (0.34 eV) Fermi level shift is obtained by −40 to 40 V gate control. (c) The simulations (Lines) and experiments (Points) of the FESBT. (d) Theoretical analysis showing that the subthreshold swing of FESBT overcomes the limitation of 60 mV/dec of conventional FET. (e) The mobility vs. the V_{gate} showing a maximum mobility of 58.7 $cm^2/V\cdot s$. The mobility is induced from the experimental results in Fig. 2c at 0.1 V bias. (f) The mobility vs. the Schottky barrier height showing that the maximum mobility is obtained at a barrier height of 0.26 eV.

In order to show the advance of our FESBT, the mobility and on/off ratio of the back-gated MoS_2 transistors[16,31–34], graphene transistors[35–37] and FESBT are compared in Figure 6. The references are selected based on their reliability and similarity to the structure of our device. Especially, we use back-gated MoS_2 transistors for comparison. Kaasbjerg et al.'s work found that the mobility of MoS_2 at room temperature is limited down to ~410 $cm^2/V\cdot s$ due to optical phonon scattering[38]. Additionally, some previous works investigated high-κ dielectric as top gate oxide, which has improved the mobility significantly[39]. The reason for the improvement of the MoS_2 mobility was due to the introduction of "imaginary charges" to suppress the scattering potential[40] and high-κ dielectric which enhanced the screening of impurity charges[39]. In order to compare with works in which a similar device structure is employed, we select the references in

Figure 5 | The energy band diagrams for GMH and MGM. (a) Schematic view of the energy level alignment of the FESBT with Si/SiO_2/MoS_2/Graphene structure. (b) Schematic band diagrams of GMH with $V_{gate} = 0$. (c) Schematic band diagram of GMH with $V_{gate} > 0$. Applying a positive voltage on the gate induces electrons in graphene, decreasing its work function and the Schottky barrier height. (d) Schematic band diagrams of GMH with $V_{gate} < 0$. Applying a negative voltage on the gate induces holes in graphene, lowering its Fermi level and increasing the Schottky barrier height. Panels (e) and (f) show the energy diagram of the MGM under different gate voltages. When a higher gate voltage is applied, it induces more charges in graphene, due to which the Fermi level rises. Thus the energy barrier between graphene and MoS_2 decreases and the conductance increases. In this way, the current flow is modulated by the gate voltage.

Figure 6 that only adopts SiO_2 as a back gate dielectric. Our FESBT has a mobility up to 58.7 $cm^2/V\cdot s$ with an on/off ratio of 10^5. Although the mobility of the graphene could be up to 10^5 $cm^2/V\cdot s$, the drawback of graphene transistors is the low on/off ratio (typically lower than 10). Most recently, MoS_2 is developed to realize ultra-high on/off ratio up to 10^8. But the state-of-the-art mobility of MoS_2 is still lower than 20 $cm^2/V\cdot s$. FESBT devices occupy a trade-off space between high mobility and considerable on-off ratio, which are separately realized by graphene transistors and MoS_2 transistors in previous works. Also as a two-dimensional device, FESBT has potential

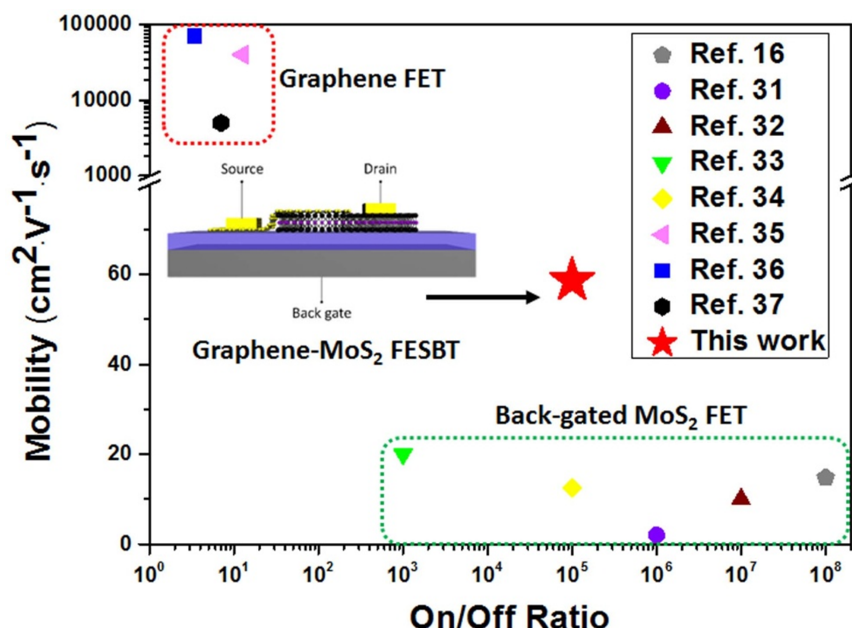

Figure 6 | Comparison of our FESBT with state-of-the-art graphene transistors and back-gated MoS_2 transistors. The graphene transistors have a high mobility but quite a low on/off ratio. The MoS_2 transistors have a high on/off ratio but quite a low mobility. The FESBT combines the qualities of high mobility from graphene and high on-off ratio from MoS_2.

in high-performance flexible electronics. Combining these advantages together with its predictable low subthreshold swing, FESBT devices should have opportunities in next-generation electronics for low-voltage, low-power and flexible applications.

Conclusion

In summary, we have demonstrated that a heterojunction of graphene and MoS_2 acts as an ideal vertical Schottky barrier, which can be tunable by field effect. The on/off ratio is as high as 10^5 with a mobility up to 58.7 $cm^2/V\cdot s$, which could meet the requirement for integrated circuit logic applications. Furthermore, the subthreshold swing is not limited by the 60 mV/decade conventional FET limit, since the field-effect Schottky barrier transistor (FESBT) has a different mechanism of gate control. A MoS_2-graphene-MoS_2 FESBT based on two GMHs is also demonstrated, which has an ability to rectify the current by changing the gate voltage. As the barrier is formed vertically, our devices could also be laterally scaled and are well-suited for low-power applications.

Experimental Section

Device fabrication. Few-layer MoS_2 and graphene flakes were in turn exfoliated on to 300-nm-thick SiO_2 on N^+ doped silicon substrate as the back-gate structure. The contacts to MoS_2 and graphene were subsequently fabricated using electron beam lithography and electron beam evaporation of Cr/Au metal (10 nm/50 nm).

Characterization. The optical image is captured using a VH-8000 microscope (KEYENCE Inc.). Raman spectroscopy is performed using a laser with a wavelength of 514.5 nm (HORIBA Inc.). The AFM images are obtained in tapping mode by using Esweep (Seiko Inc.).

Transport measurements. The I–V characteristics of the FESBT were measured by a standard probe station (Agilent Inc. B1500) at room temperature (300 K).

1. Geim, A. K. & Novoselov, K. S. The rise of graphene. *Nat. Mater.* **6**, 183–191 (2007).
2. Novoselov, K. *et al.* Electric field effect in atomically thin carbon films. *Science* **306**, 666–669 (2004).
3. Bolotin, K. I. *et al.* Ultrahigh electron mobility in suspended graphene. *Solid State Commun.* **146**, 351–355 (2008).
4. Lee, C., Wei, X., Kysar, J. W. & Hone, J. Measurement of the elastic properties and intrinsic strength of monolayer graphene. *Science* **321**, 385–388 (2008).
5. Balandin, A. A. *et al.* Superior thermal conductivity of single-layer graphene. *Nano Lett.* **8**, 902–907 (2008).
6. Tian, H. *et al.* Single-layer graphene sound-emitting devices: experiments and modeling. *Nanoscale* **4**, 2272–2277 (2012).
7. Li, X., Wang, X., Zhang, L., Lee, S. & Dai, H. Chemically derived, ultrasmooth graphene nanoribbon semiconductors. *Science* **319**, 1229–1232 (2008).
8. Wang, X. *et al.* Room-temperature all-semiconducting sub-10-nm graphene nanoribbon field-effect transistors. *Phys. Rev. Lett.* **100**, 206803 (2008).
9. Castro, E. V. *et al.* Biased bilayer graphene: semiconductor with a gap tunable by the electric field effect. *Phys. Rev. Lett.* **99**, 216802 (2007).
10. Zhang, Y. *et al.* Direct observation of a widely tunable bandgap in bilayer graphene. *Nature* **459**, 820–823 (2009).
11. Dikin, D. A. *et al.* Preparation and characterization of graphene oxide paper. *Nature* **448**, 457–460 (2007).
12. Tian, H. *et al.* A novel flexible capacitive touch pad based on graphene oxide film. *Nanoscale* **5**, 890–894 (2013).
13. Novoselov, K. *et al.* Two-dimensional atomic crystals. *Proc. Natl. Acad. Sci. U. S. A.* **102**, 10451–10453 (2005).
14. Radisavljevic, B. & Kis, A. Reply to 'Measurement of mobility in dual-gated MoS2 transistors'. *Nat. Nanotechnol.* **8**, 147–148 (2013).
15. Yin, Z. *et al.* Single-layer MoS2 phototransistors. *ACS Nano* **6**, 74–80 (2011).
16. Pu, J. *et al.* Highly flexible MoS2 thin-film transistors with ion gel dielectrics. *Nano Lett.* **12**, 4013–4017 (2012).
17. Haigh, S. *et al.* Cross-sectional imaging of individual layers and buried interfaces of graphene-based heterostructures and superlattices. *Nat. Mater.* **11**, 764–767 (2012).
18. Britnell, L. *et al.* Field-effect tunneling transistor based on vertical graphene heterostructures. *Science* **335**, 947–950 (2012).
19. Georgiou, T. *et al.* Vertical field-effect transistor based on graphene-WS2 heterostructures for flexible and transparent electronics. *Nat. Nanotechnol.* **8**, 100–103 (2012).
20. Zhang, W. *et al.* Ultrahigh-Gain Phototransistors Based on Graphene-MoS2 Heterostructures. *arXiv preprint arXiv:13021230* (2013).
21. Yu, W. J. *et al.* Vertically stacked multi-heterostructures of layered materials for logic transistors and complementary inverters. *Nat. Mater.* **12**, 246–252 (2012).
22. Yu, W. J. *et al.* Highly efficient gate-tunable photocurrent generation in vertical heterostructures of layered materials. *Nat. Nanotechnol.* **8**, 952–958 (2013).
23. Bertolazzi, S., Krasnozhon, D. & Kis, A. Nonvolatile memory cells based on MoS2/graphene heterostructures. *ACS Nano* **7**, 3246–3252 (2013).
24. Choi, M. S. *et al.* Controlled charge trapping by molybdenum disulphide and graphene in ultrathin heterostructured memory devices. *Nat. Commun.* **4**, 1624 (2013).

25. Roy, K. *et al*. Graphene-MoS2 hybrid structures for multifunctional photoresponsive memory devices. *Nat. Nanotechnol.* **8**, 826–830 (2013).
26. Yu, W. J. *et al*. Vertically stacked multi-heterostructures of layered materials for logic transistors and complementary inverters. *Nat. Mater.* **12**, 246–252 (2013).
27. Heinze, S. *et al.* Carbon nanotubes as Schottky barrier transistors. *Phys. Rev. Lett.* **89**, 106801 (2002).
28. Larson, J. M. & Snyder, J. P. Overview and status of metal S/D Schottky-barrier MOSFET technology. *IEEE Trans. Electron Devices* **53**, 1048–1058 (2006).
29. Yang, H. *et al*. Graphene barristor, a triode device with a gate-controlled Schottky barrier. *Science* **336**, 1140–1143 (2012).
30. Cheung, K. On the 60 mV/dec@ 300 K limit for MOSFET subthreshold swing. *Int. Symp. VLSI Technol., Syst., Appl. (VLSI-TSA)*, pp.72–73 (2010).
31. Radisavljevic, B. & Kis, A. Mobility engineering and a metal-insulator transition in monolayer MoS2. *Nat. Mater.* **12**, 815–820 (2013).
32. Liu, K.-K. *et al*. Growth of Large-Area and Highly Crystalline MoS2 Thin Layers on Insulating Substrates. *Nano Lett.* **12**, 1538–1544 (2012).
33. Wang, H. *et al*. Integrated Circuits Based on Bilayer MoS2 Transistors. *Nano Lett.* **12**, 4674–4680 (2012).
34. Ghatak, S., Pal, A. N. & Ghosh, A. Nature of Electronic States in Atomically Thin MoS2 Field-Effect Transistors. *ACS Nano* **5**, 7707–7712 (2011).
35. Chen, J.-H., Jang, C., Xiao, S., Ishigami, M. & Fuhrer, M. S. Intrinsic and extrinsic performance limits of graphene devices on SiO2. *Nat. Nanotechnol.* **3**, 206–209 (2008).
36. Chen, F., Xia, J., Ferry, D. K. & Tao, N. Dielectric Screening Enhanced Performance in Graphene FET. *Nano Lett.* **9**, 2571–2574 (2009).
37. Kedzierski, J. *et al*. Epitaxial graphene transistors on SiC substrates. *IEEE Trans. Electron Devices* **55**, 2078–2085 (2008).
38. Kaasbjerg, K., Thygesen, K. S. & Jacobsen, K. W. Phonon-limited mobility in n-type single-layer MoS_ {2} from first principles. *Phys. Rev. B* **85**, 115317 (2012).
39. Radisavljevic, B., Radenovic, A., Brivio, J., Giacometti, V. & Kis, A. Single-layer MoS2 transistors. *Nat. Nanotechnol.* **6**, 147–150 (2011).
40. Jena, D. & Konar, A. Enhancement of carrier mobility in semiconductor nanostructures by dielectric engineering. *Phys. Rev. Lett.* **98**, 136805 (2007).

Acknowledgments

He Tian, Zhen Tan, Can Wu and Xiaomu Wang contributed equally to this work. This work was supported by the National Natural Science Foundation of China (61025021, 60936002, 51072089, and 61020106006), the National Science and Technology Major Project (2011ZX02403-002, 2011ZX02708-002), the State Key Development Program for Basic Research of China (No. 2011CBA00602)) and the Special Fund for Agro-scientific Research in the Public Interest (201303107). He Tian is additionally supported by the Ministry of Education Scholarship of China. M.A.M. is additionally supported by the postdoctoral fellowship (PDF) program of the Natural Sciences and Engineering Research Council of Canada (NSERC). Thanks for the valuable discussions with Professor H.-S. Philip Wong from Stanford University and Professor Wenhui Duan from Tsinghua University.

Author contributions

H.T. and Z.T. made and tested the samples and drafted the manuscript. C.W. and X.W. performed simulations. H.T., Z.T., C.W. and X.W. contributed equally to this work. T.-L.R., J.X. and L.-J.L. oversaw all research phases, optimized the devices performance and revised the manuscript. M.A.M., D.X., Y.Y. and J.W. analyzed the test results and revised the manuscript. All authors discussed and commented on the manuscript.

Additional information

Supplementary information accompanies this paper at http://www.nature.com/scientificreports

Competing financial interests: The authors declare no competing financial interests.

How to cite this article: Tian, H. *et al.* Novel Field-Effect Schottky Barrier Transistors Based on Graphene-MoS_2 Heterojunctions. *Sci. Rep.* **4**, 5951; DOI:10.1038/srep05951 (2014).

This work is licensed under a Creative Commons Attribution-NonCommercial-NoDerivs 4.0 International License. The images or other third party material in this article are included in the article's Creative Commons license, unless indicated otherwise in the credit line; if the material is not included under the Creative Commons license, users will need to obtain permission from the license holder in order to reproduce the material. To view a copy of this license, visit http://creativecommons.org/licenses/by-nc-nd/4.0/